Chimera Grid Method for Incompressible Flows and its Applications in Actual Problems

H. S. Tang

Dept. of Civil Eng., City College
City Univ. of New York

Collaborators: C. H. Lee, T. Zhou,
Sotiropoulos, J. Paik, X. G. Wu

10th Symposium on Overset Composite Grids and Solution Technology
NASA Ames Research Center, CA
Sept. 20-23, 2010

the City College of New York

Outline

I. Introduction
II. Grid interface algorithms
III. Incompressible flows
III. Environmental flows
IV. Coastal ocean flows
V. Concluding remarks

Domain decomposition and Chimera grids

Advantages

- Overcome difficulty in mesh generation
- Utilize parallel computation approaches
- Attack multi-scale and multi-physics problems

Grid/Model Interface Treatment --- Crucial Issue

- Conservative algorithms – difficult to realize, unstable, inconsistency, ...
- Non-conservative algorithms – easy to realize, wrong solution, numerical oscillation, ….

II. Grid Interface Algorithm

Conservative or non-conservative treatment?

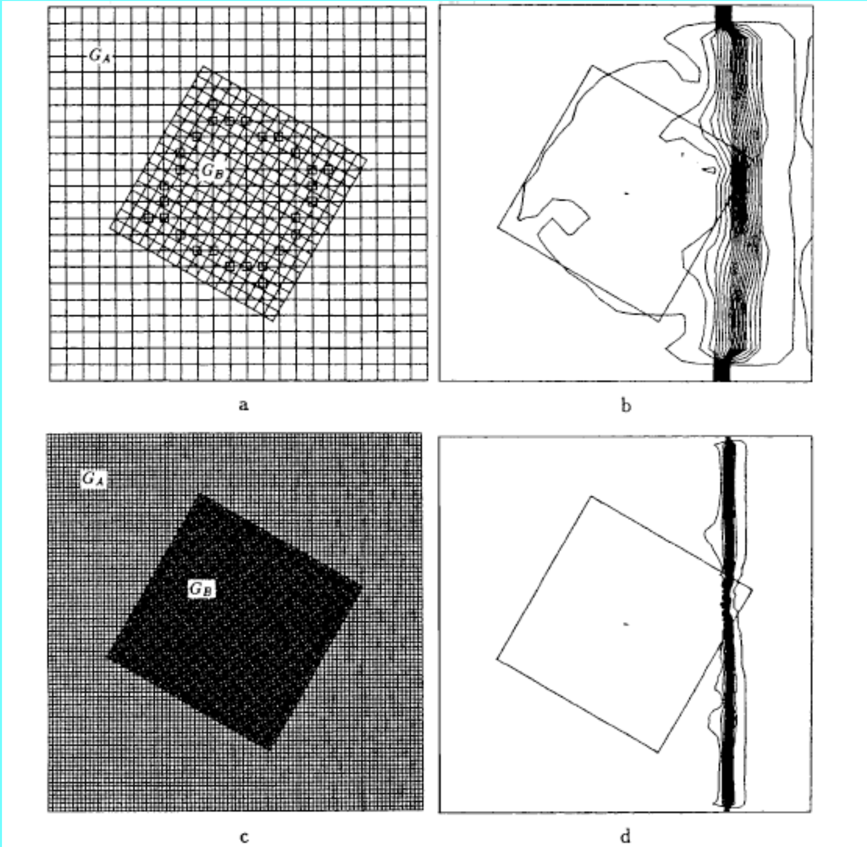

Physical solution obtained with bi-linear interpolation at grid interface

It is proven that numerical solution converges to a weak solution under certain conditions if a non-conservative interface algorithm is used

FIG. 4.3. *Computed results of flowfield with a shock moving to the right and passing through a square grid.* $\rho_l = 3.948$, $u_l = 4.359$, $p_l = 5.005$, $\rho_r = 1.4$, $u_r = 3$, $p_r = 1$, $T = 0.13$. *Here subscript* l *and* r *indicate left and right side, respectively.* (4.3) *is adopted at the interface nodes, a scheme based on TVNI* [18] *is used within the each grid, and* $CFL = 0.95$. (a) *Mesh arrangement.* G_A: 24×24, G_B: 18×18. (b) *Pressure contours for* (a), $\|S_{2\Delta}(0,T)\|_\infty = 2.4 \times 10^{-3}$. (c) *Mesh arrangement.* G_A: 93×93, G_B: 69×69. (d) *Pressure contours for* (c), $\|S_{2\Delta}(0,T)\|_\infty = 7.1 \times 10^{-5}$.

II. Grid Interface Algorithm

Conservative or non-conservative treatment?

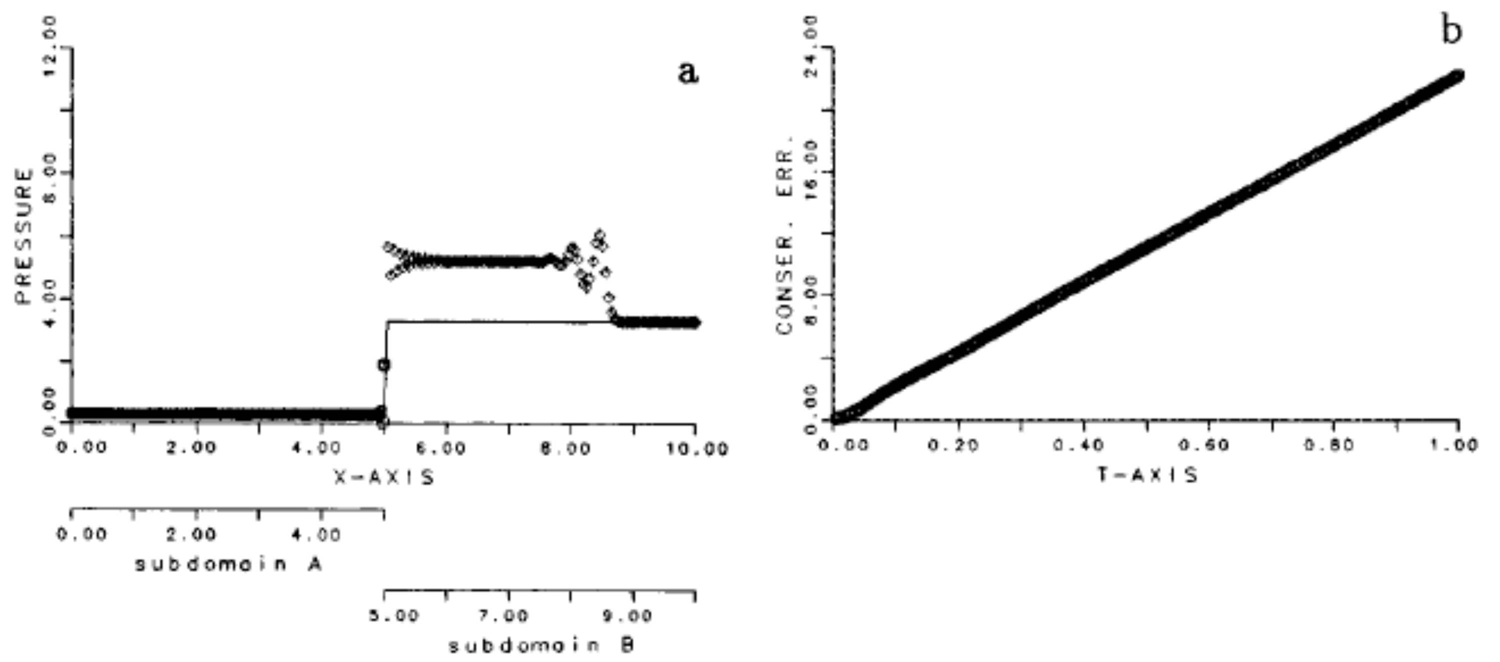

FIG. 4.4. *A steady shock is located at the interface. Initially when* $x < 0$, $\rho = 0.25$, $u = 4$, $p = 0.2857142$, *and when* $x > 0$, $\rho = 1$, $u = 1$, $p = 3.2857142$. $T = 1$. *Interface scheme is* (2.4). *The Lax–Wendroff scheme is adopted in both subdomains A and B*, $\Delta x_A = 0.025$, $\Delta x_B = 0.05$, $CFL = 0.95$. (a) *Pressure solutions. Dots—numerical results, solid line—exact solution.* (b) *History of conservation error* $\|S_{1\Delta}(0,t)\|_\infty$.

Non-physical solution obtained with linear interpolation

A mass conservation algorithm for incompressible flow

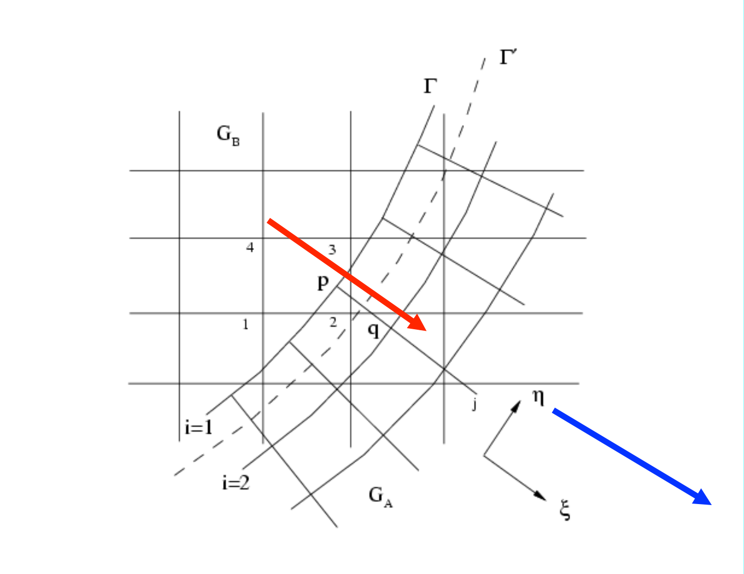

Implicit interface conditions implemented by Schwarz alternative iteration (1869)

An conservative interpolation

$$\sum_j \tilde{F}^1_{3/2,j}(U^A_p, U^A_q)\Delta\Gamma'_j = \sum_j \tilde{F}^1_{3/2,j}(U^B_p, U^B_q)\Delta\Gamma'_j,$$

Algorithm 1

$$U^{\mathrm{A}}_{1,j,k} = J_{1,j,k}\left(\left(\frac{U^{\mathrm{I}}}{J}\right)_{1,j,k} + \left(\frac{U^{\mathrm{I}}}{J}\right)_{2,j,k} - \left(\frac{U^{\mathrm{A}}}{J}\right)_{2,j,k}\right),$$
$$V^{\mathrm{A}}_{1,j,k} = V^{\mathrm{I}}_{1,j,k},$$
$$W^{\mathrm{A}}_{1,j,k} = W^{\mathrm{I}}_{1,j,k},$$
$$p^{\mathrm{A}}_{1,j,k} = p^{\mathrm{I}}_{1,j,k}.$$

Algorithm 2

$$u^{\mathrm{A}}_{1,j,k} = u^{\mathrm{I}}_{1,j,k} + u^{\mathrm{I}}_{2,j,k} - u^{\mathrm{A}}_{2,j,k},$$
$$v^{\mathrm{A}}_{1,j,k} = v^{\mathrm{I}}_{1,j,k} + v^{\mathrm{I}}_{2,j,k} - v^{\mathrm{A}}_{2,j,k},$$
$$w^{\mathrm{A}}_{1,j,k} = w^{\mathrm{I}}_{1,j,k} + w^{\mathrm{I}}_{2,j,k} - w^{\mathrm{A}}_{2,j,k},$$
$$p^{\mathrm{A}}_{1,j,k} = p^{\mathrm{I}}_{1,j,k}.$$

Algorithm 1 and 2:

2nd-order accurate in conservation of mass and momentum fluxes

Incompressible – numerical experiment

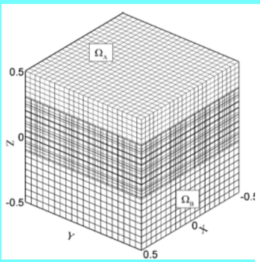

Oscillatory

cavity flow

new old

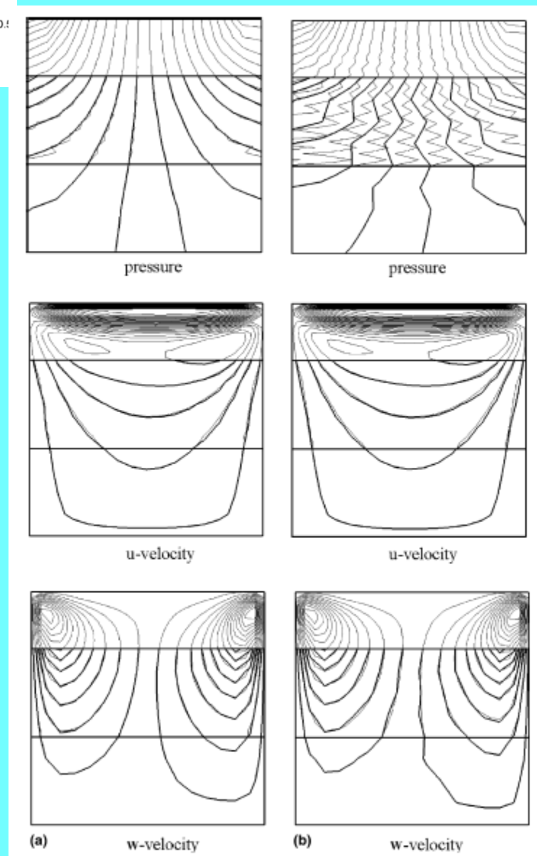

t=0.25

new old

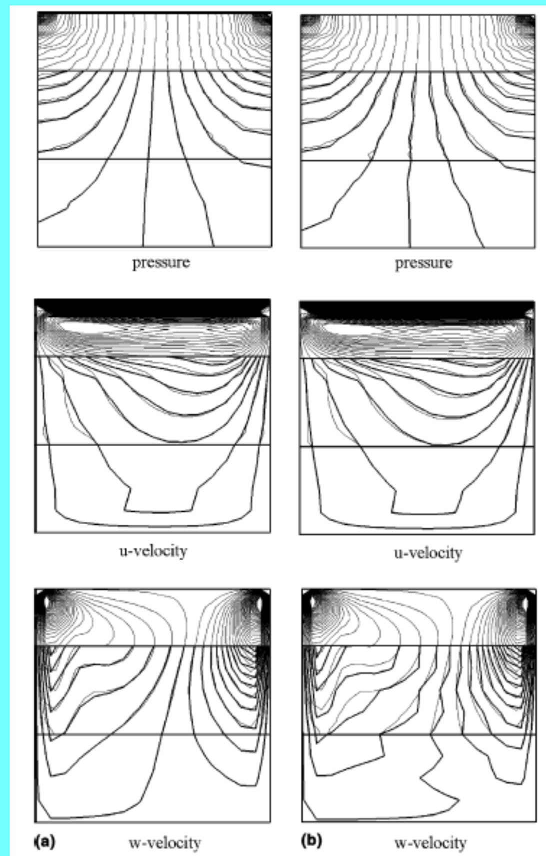

t=10

Convergence,

conservation error

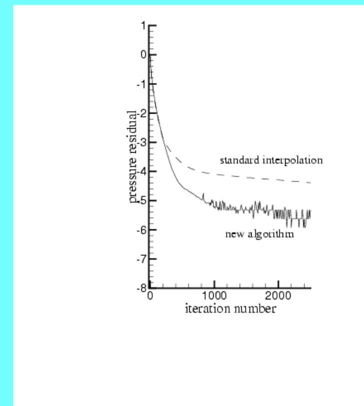

Convergence history for periodic cavity flow

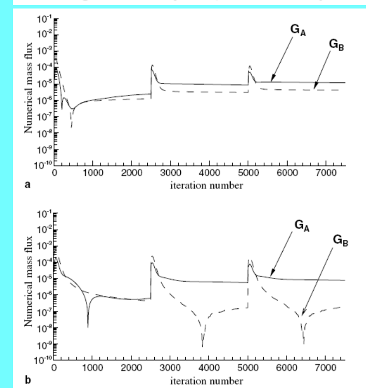

Numerical mass flux across the boundary of grid G_B. (a) MFBI and (b) SI

Incompressible – numerical experiment

Pipe bend flow

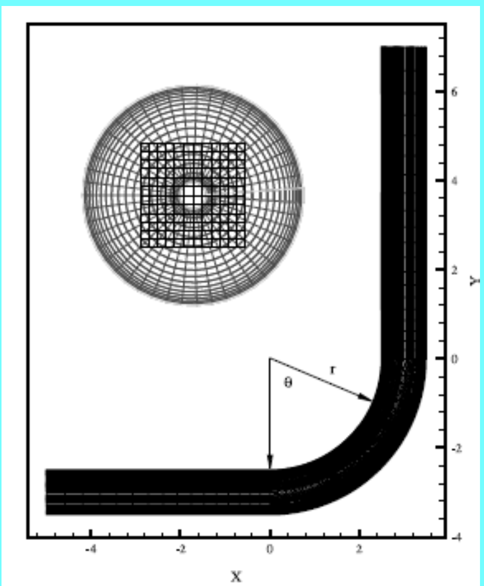

Horizontal symmetrical plane streamline velocity (computation – line, experiment – circle)

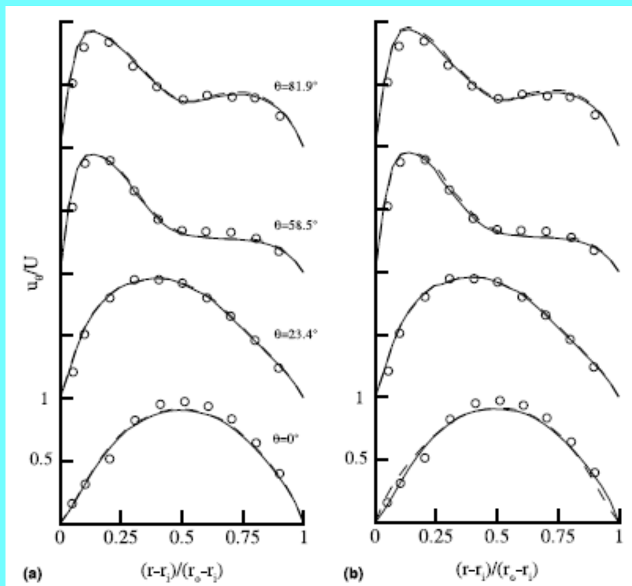

new old

Cross section pressure (top), streamline velocity (bottom)

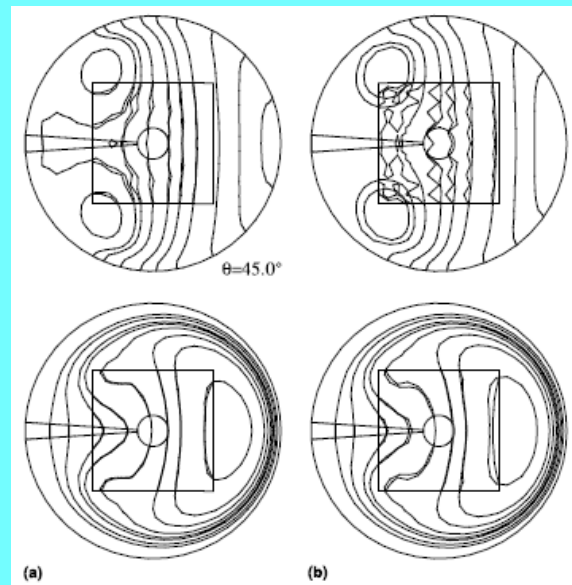

new old

Flow past cylinder – flow field

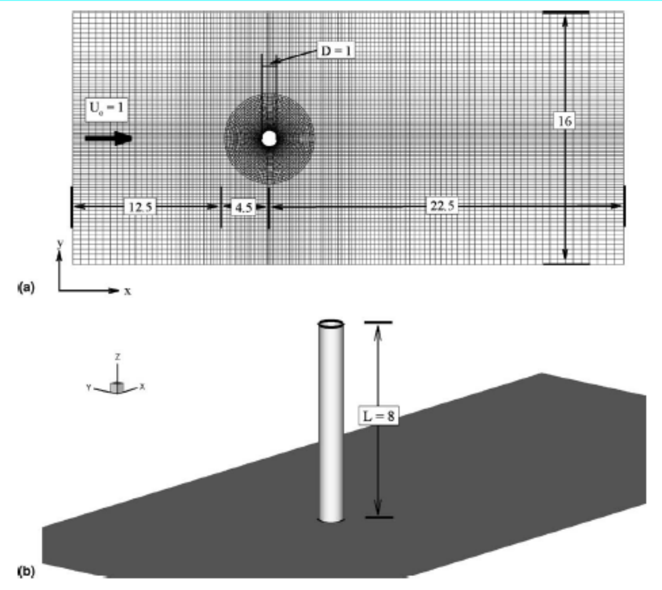

Configuration
and meshes

Re=300

x-vorticity

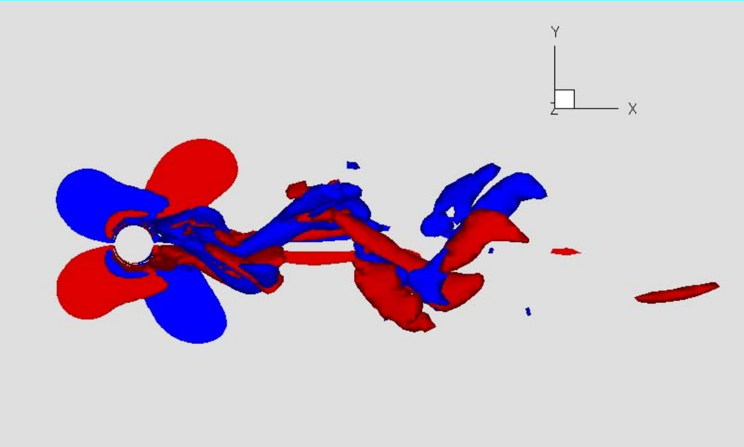

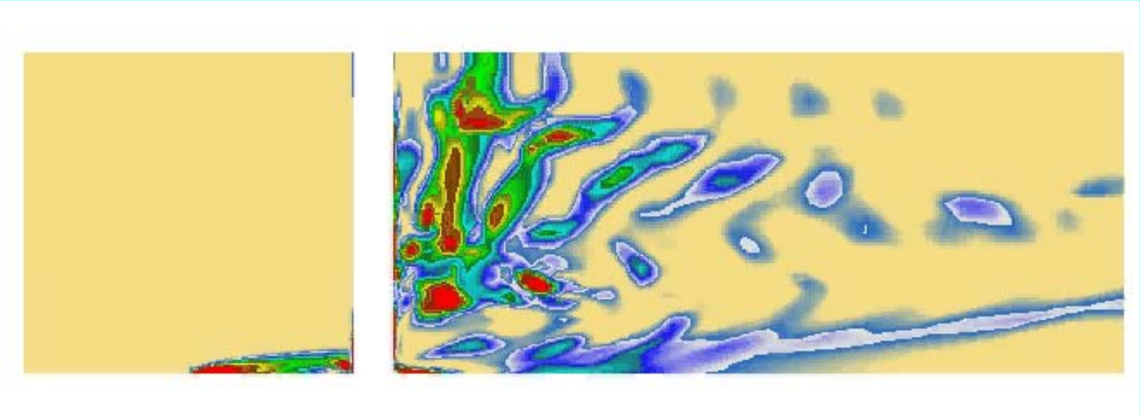

y-vorticity

III Incompressible Flow

Flow past cylinder --- comparisons

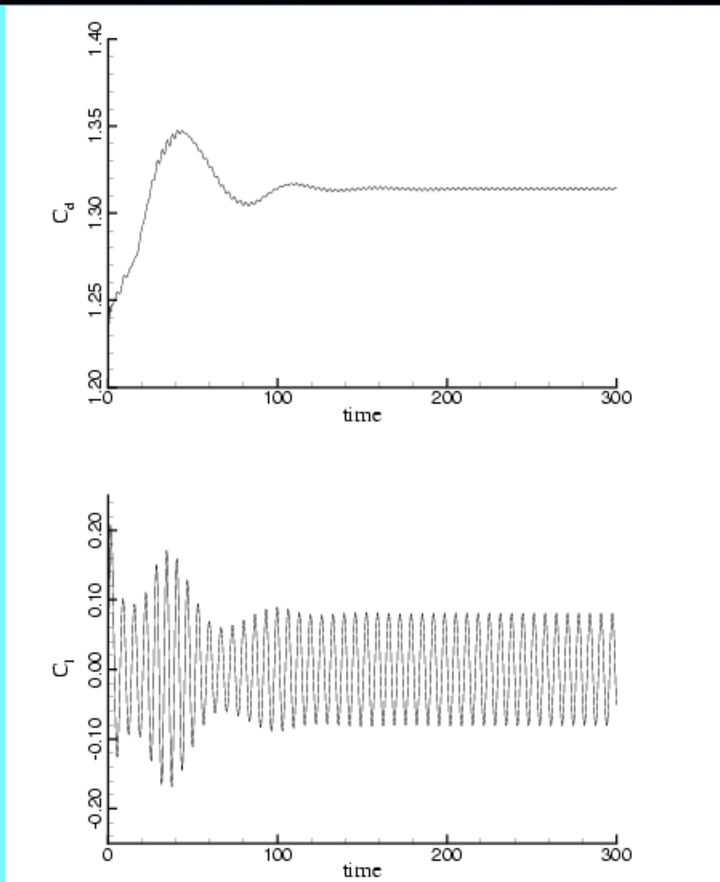

Re=100

St=0.152 Our result
=0.145 Mittal, Phys. Fluids, v13, 2001
=0.141 – 0.161 Norberg, F. Fluid Mech., v258, 1994

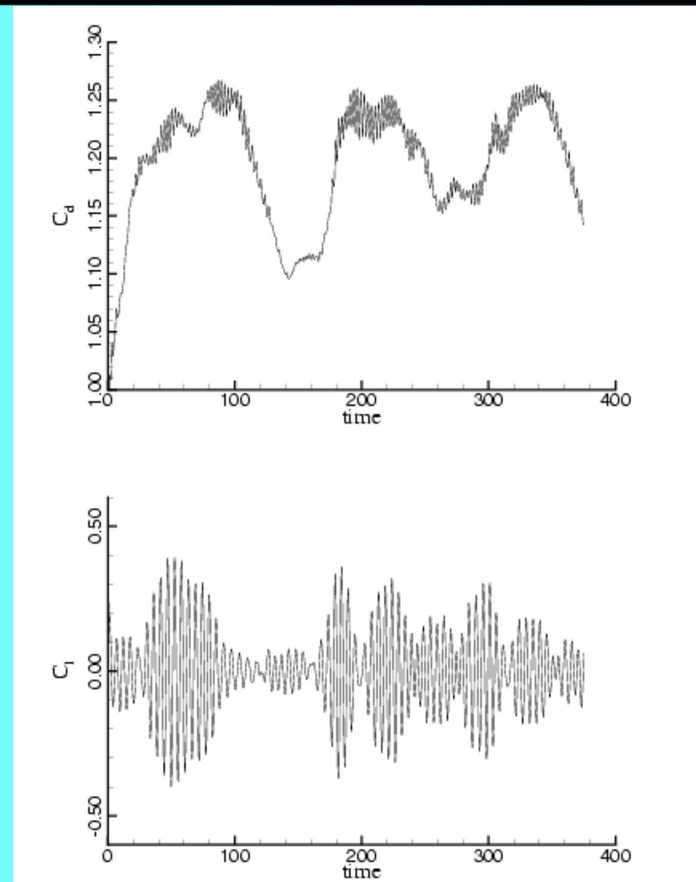

Re=300

St=0.195 Our result
=0.190 Mittal, Phys. Fluids, v13, 2001

Flow past wall-mounted structures

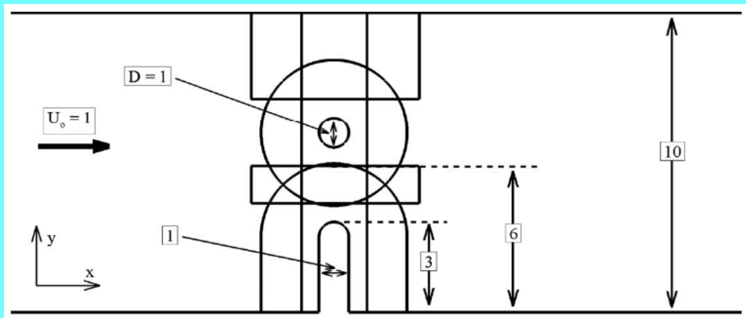

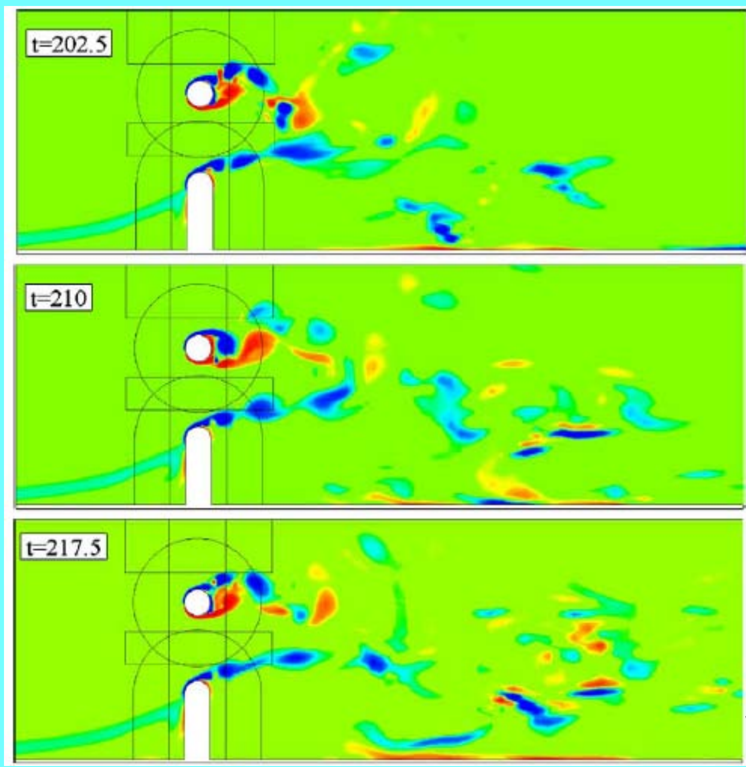

Re=300

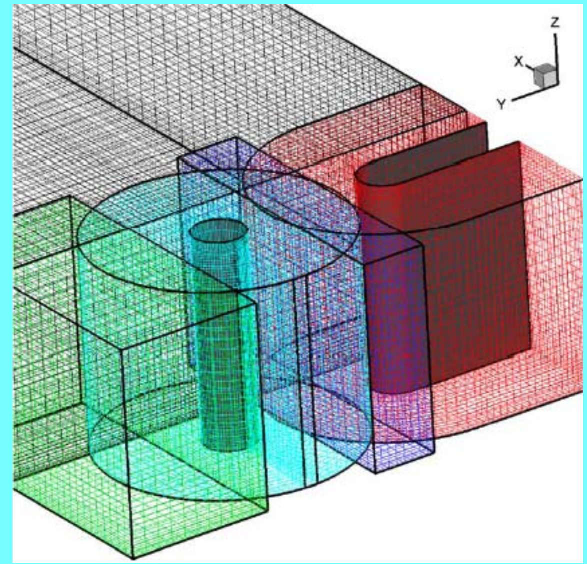

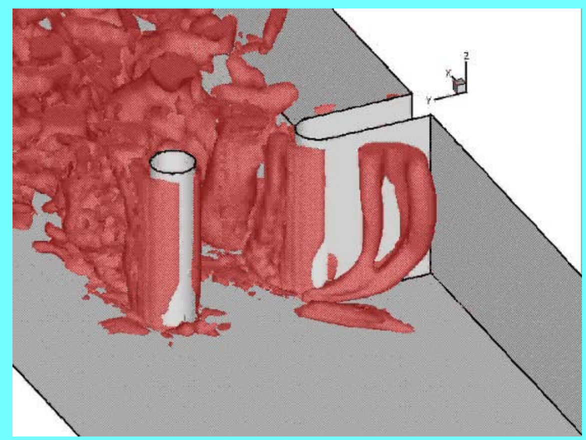

3D vortex structure (□ 2 iso-surface)

Thermal plume in natural river – flow parameter

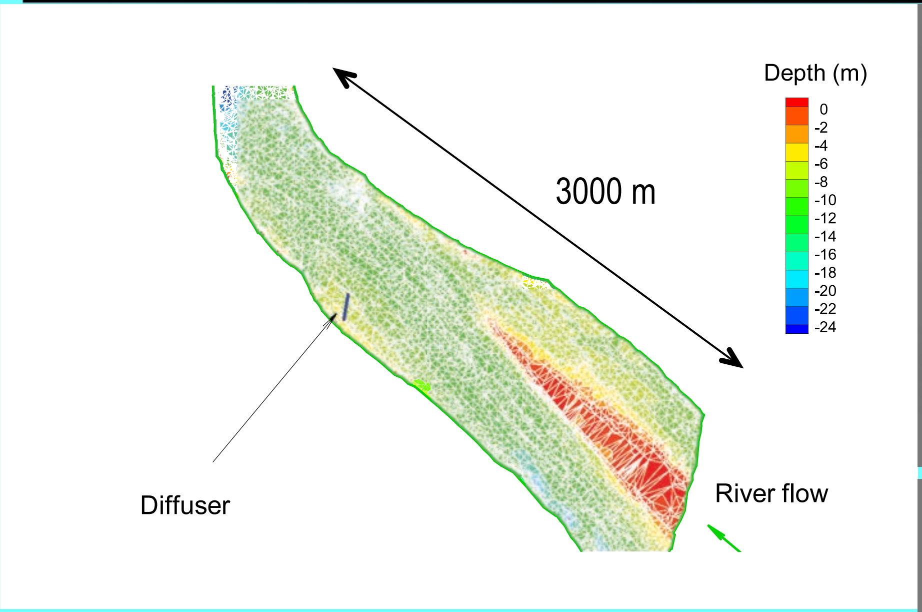

bathymetry

Ambient velocity: 0.5 m/s
Effluent velocity: 2 -- 4 m/s
Port diameters: 0.1—0.3 m

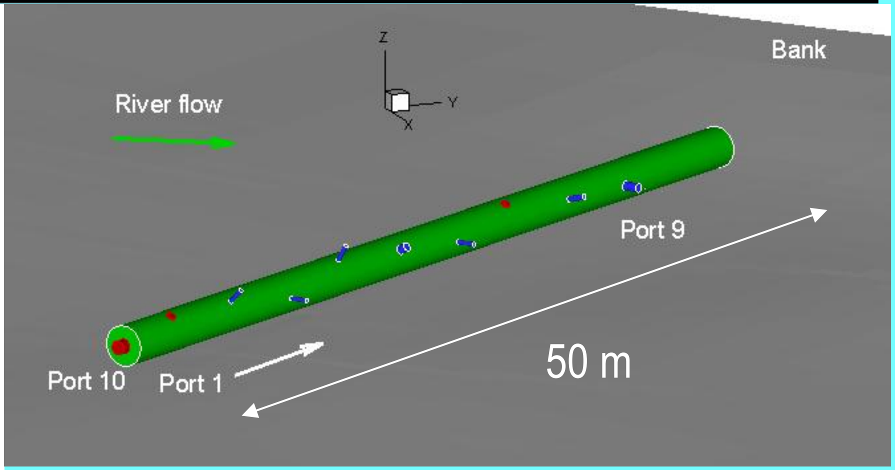

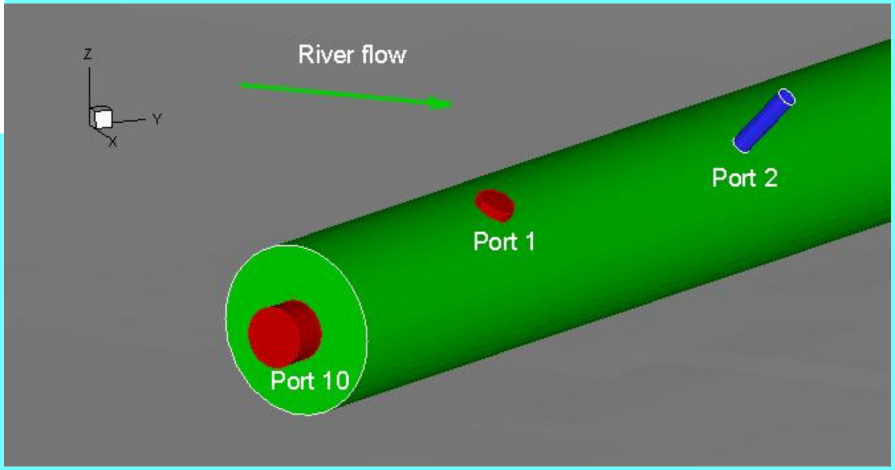

Close-up view of diffuser

Thermal plume in natural river – Chimera overset grids

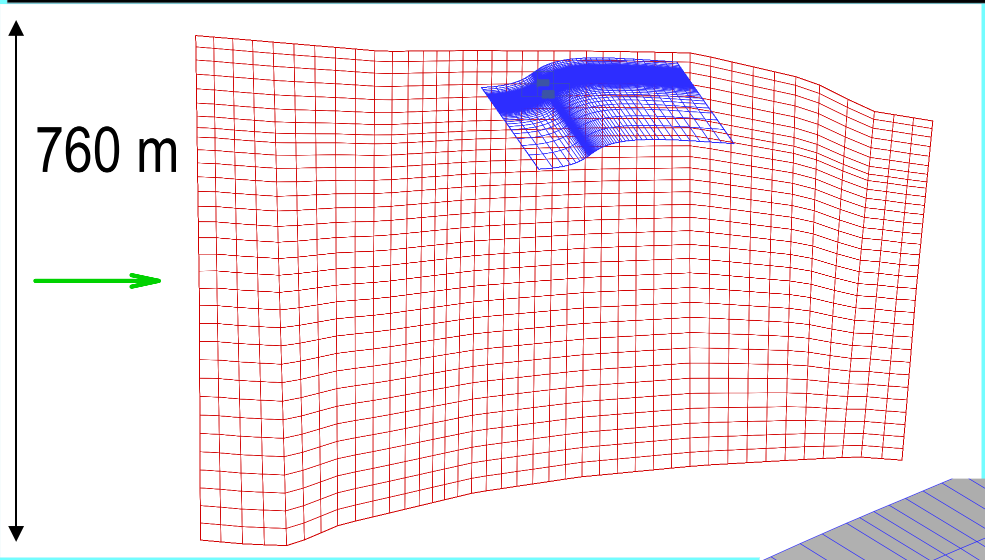

Background mesh
for river and diffusers

Zoom in mesh

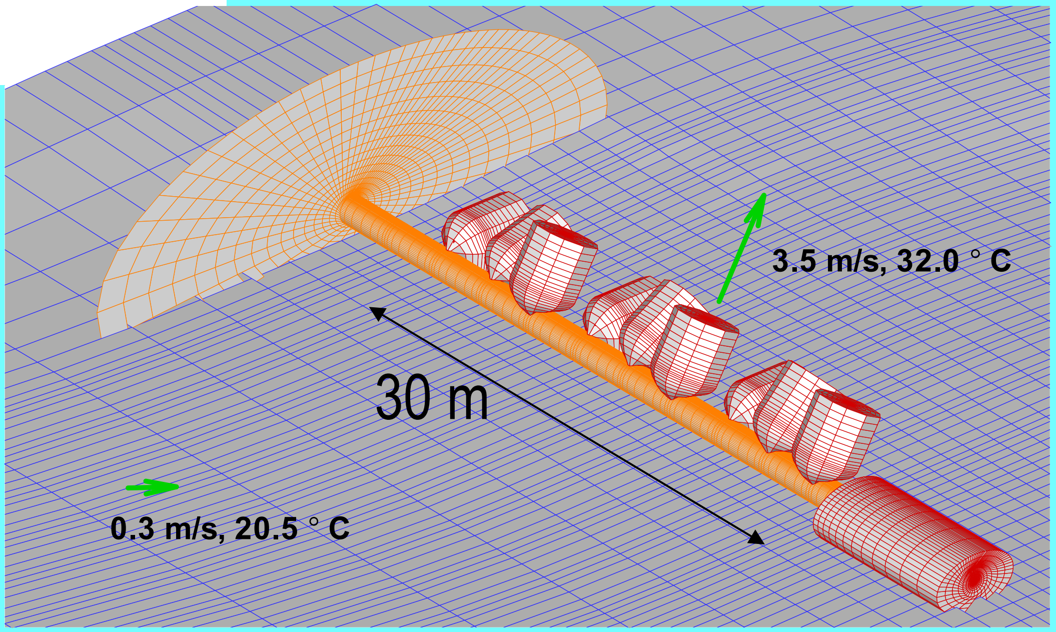

Total number of nodes
300,000

Thermal plume in natural river – solutions

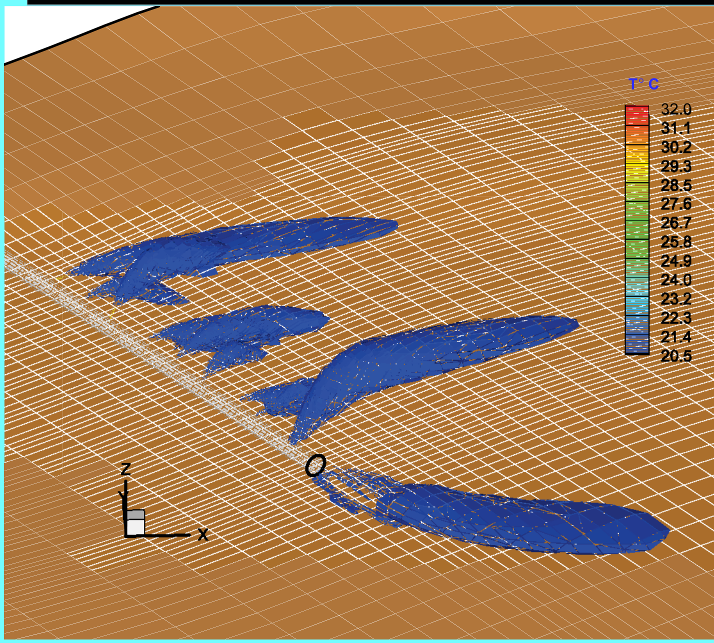

3D view of plumes
(temperature iso-surfaces)

Individual plume

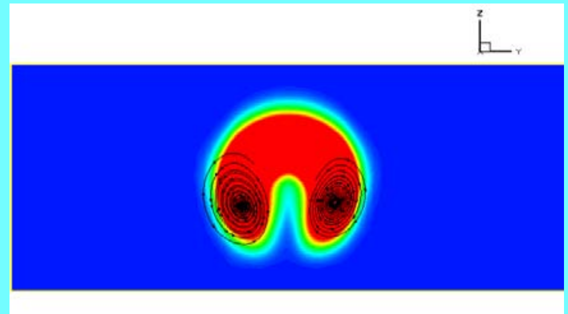

Particle tracking (movie)

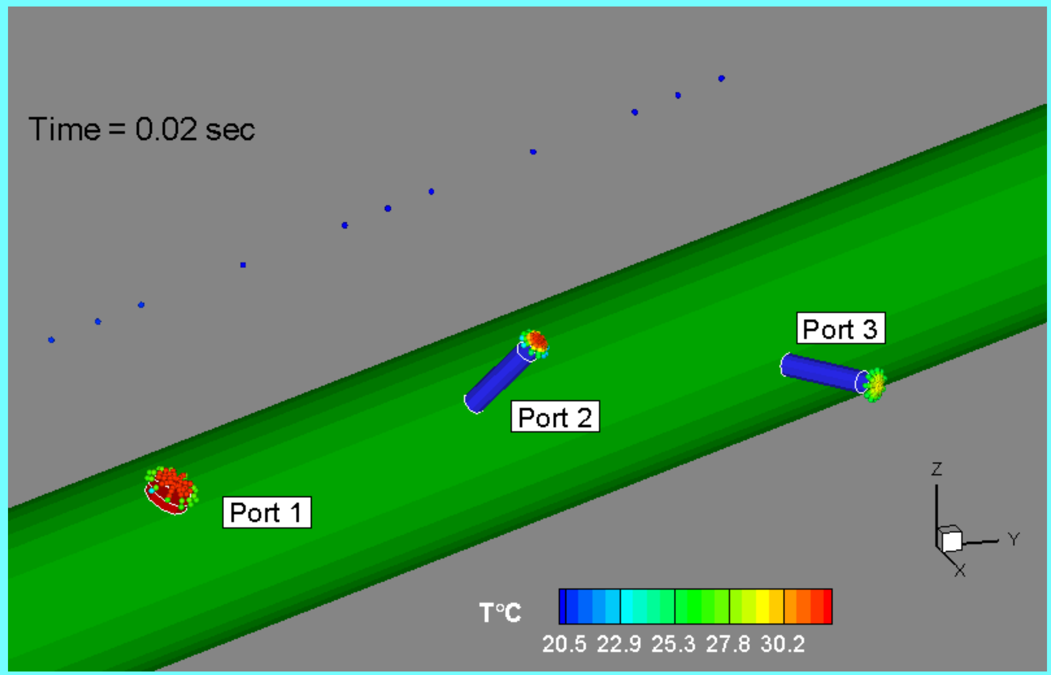

Thermal plume in natural river – predicted jets

Effluent velocity at port mouths

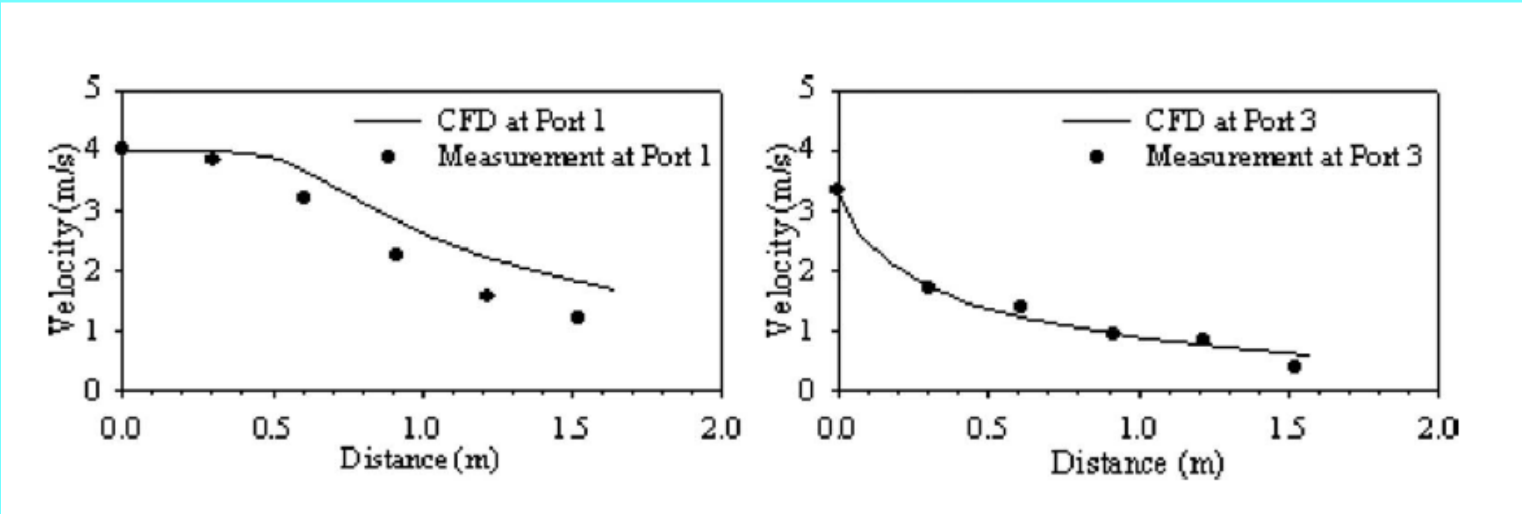

Time histories of particle temperature

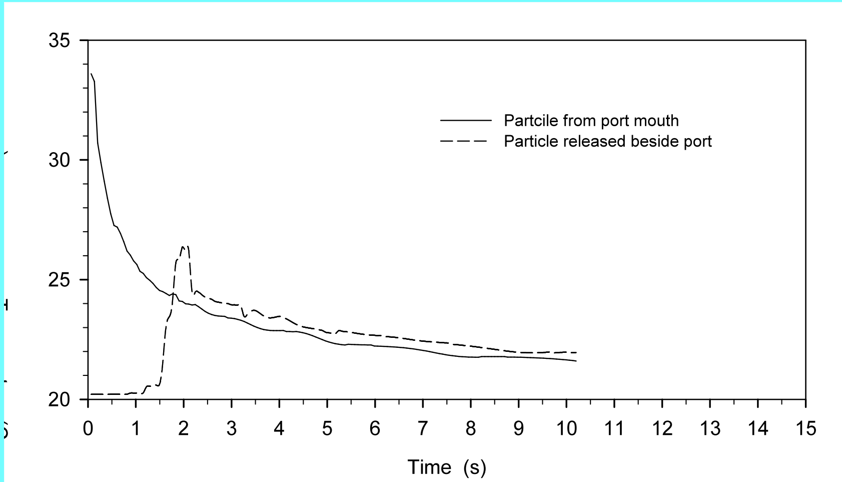

Background and models

- Large scales -- Computational Geophysics Dynamics (GFD):
  O(10)km – O (10,000) km,
  O(1)hr – O (1) month

  Note: Computational Fluid Dynamics (CFD):
  Smaller scales: O(10) cm – O (10) km
  O(1) ms – O (1) hr
  Individual phenomena: circulation, wave, etc.

- CFD model --- Unsteady, 3D, incompressible RANS, curvilinear coordinates, structured grids, finite volume method

  FVCOM --- Unsteady, 3D, incompressible GFD equations, triangular mesh in horizontal direction, sigma coordinates in vertical direction, finite volume method

Strategies -- examples

Discharge in ocean

1) small-scale initial plume of oil spill
2) large scale-floating dispersion

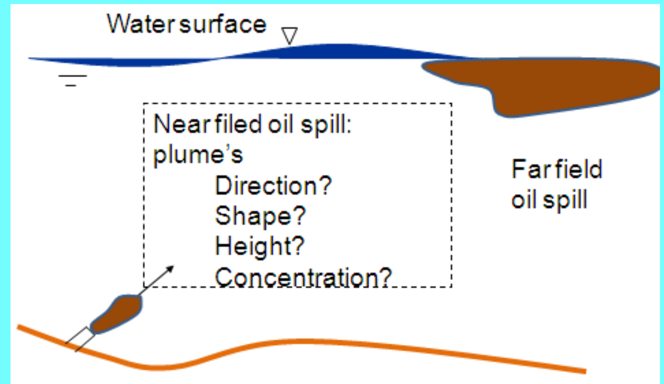

Coast process

1) surge bore
2) underwater vortex flow

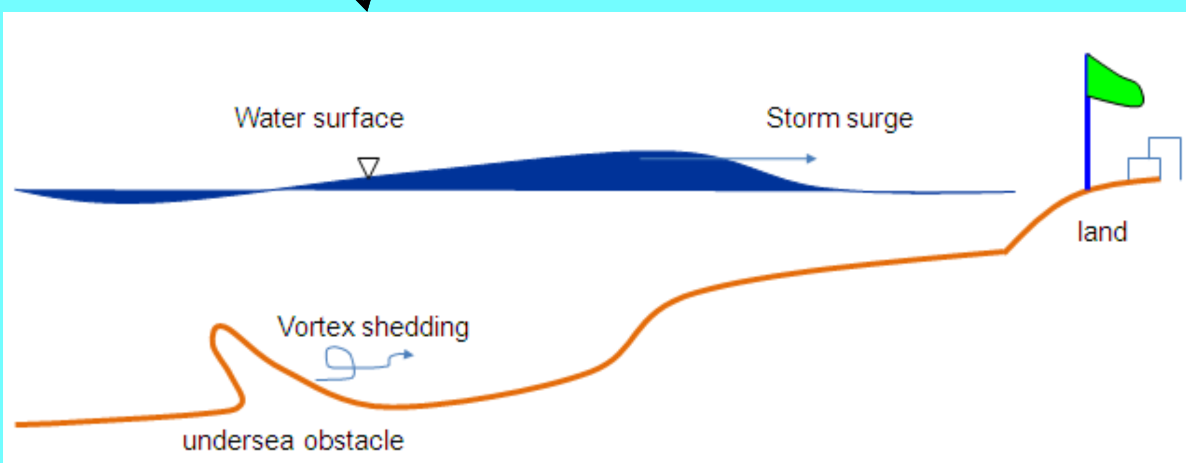

Model coupling

Flow domain decomposition
--- with overlap subdomains

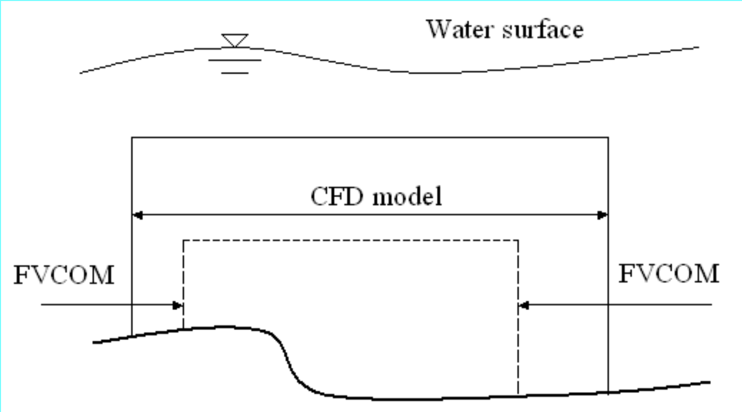

Coupling between CFD and internal mode of FVCOM --- exchange of solution for u, v, w, p/η

Chimera overset grids and
Schwarz alternative iteration

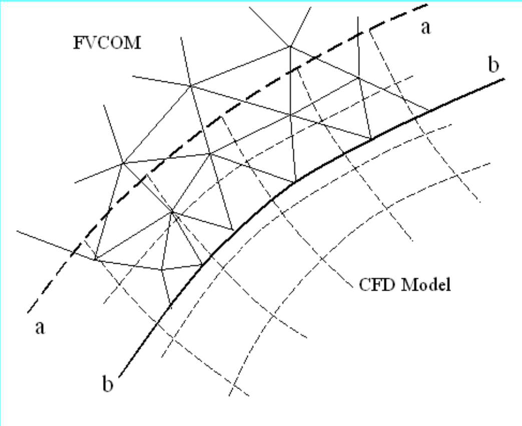

Second-order accurate interpolation at model interface

Discharge into channel --- mesh

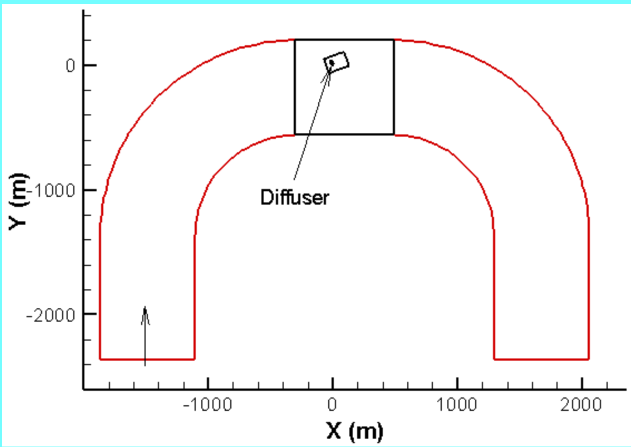

Channel and diffuser

Mesh:
coupling – FVCOM: 115,000 nodes each layer,11 layers
CFD -- 220,000 nodes

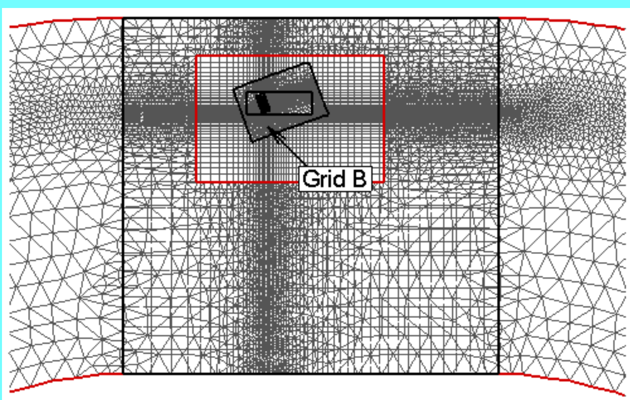

Mesh. Structured mesh – CFD
unstructured mesh – FVCOM

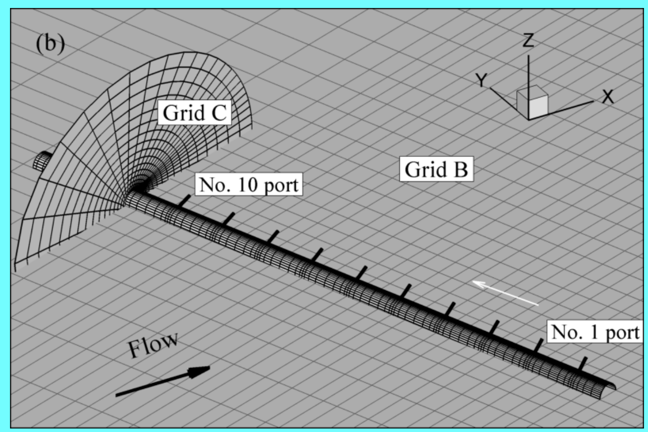

Mesh around the diffuser

Discharge into channel --- results

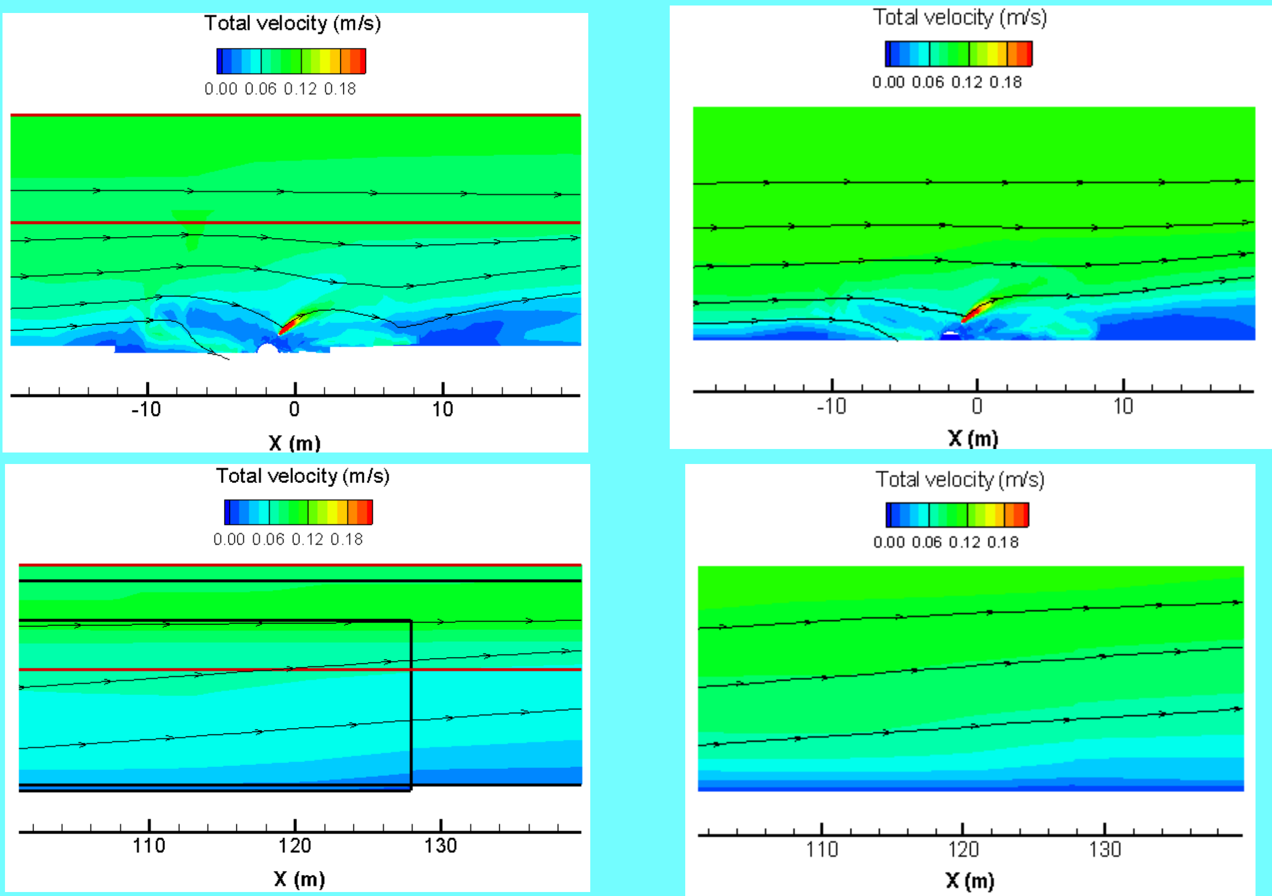

FVCOM/CFD coupling

CFD

Discharge into channel --- results

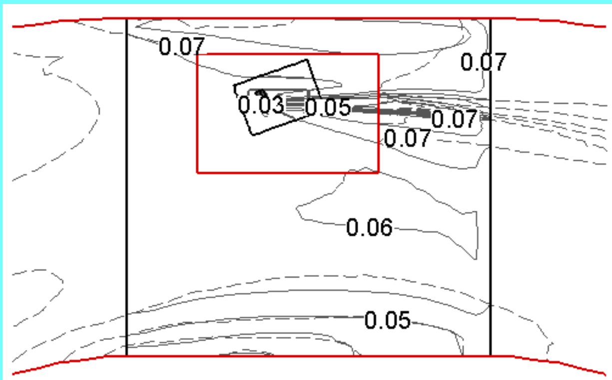

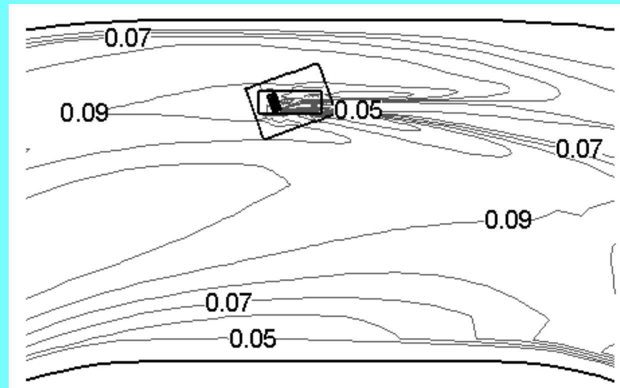

Total velocity (m/s)

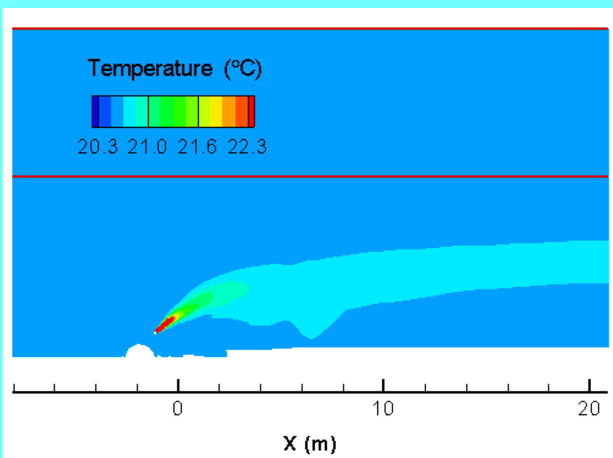

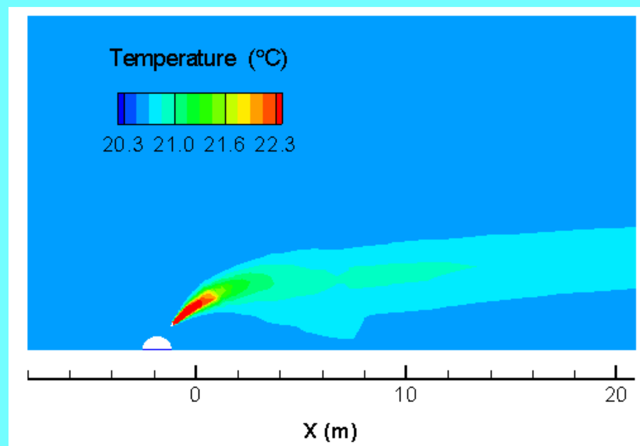

Temperature

FVCOM/CFD coupling

CFD

Discharge into coastal flow --- mesh

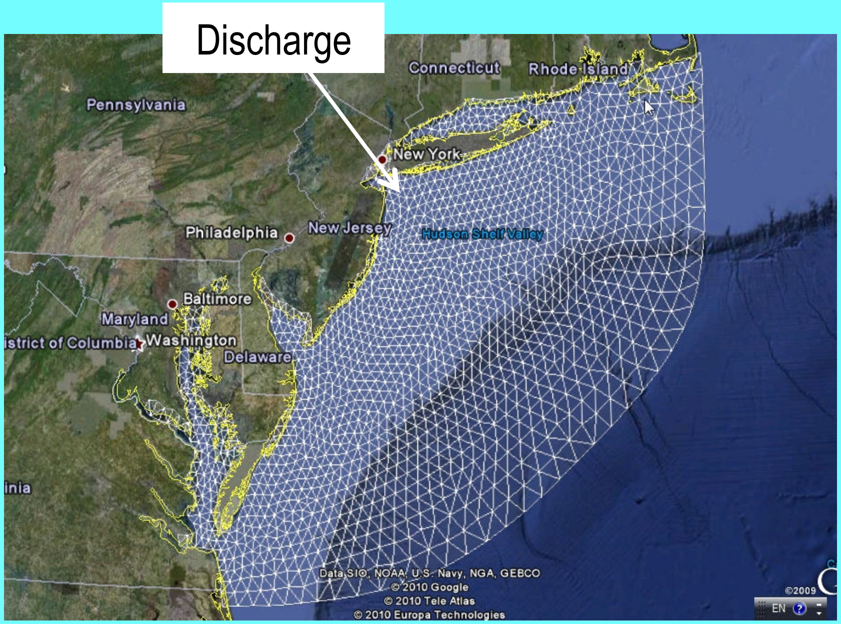

FVCOM mesh and CFD location

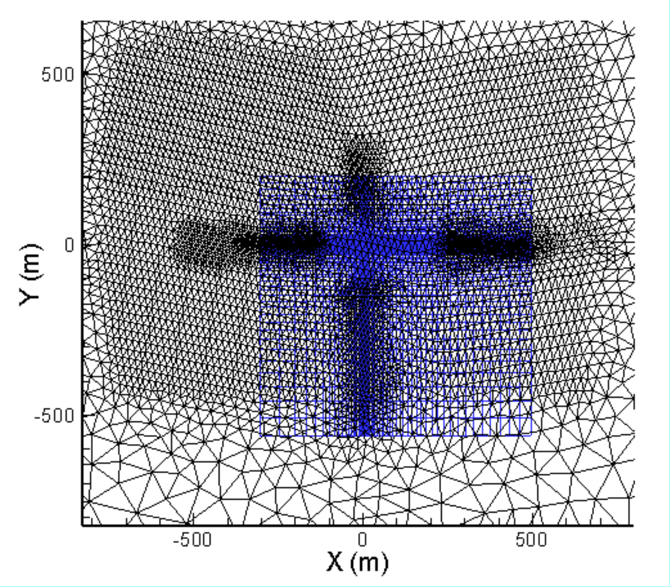

CFD mesh (blue)

New York/New Jersey coast region and FVCOM mesh and CFD location

Discharge into coastal flow --- solutions

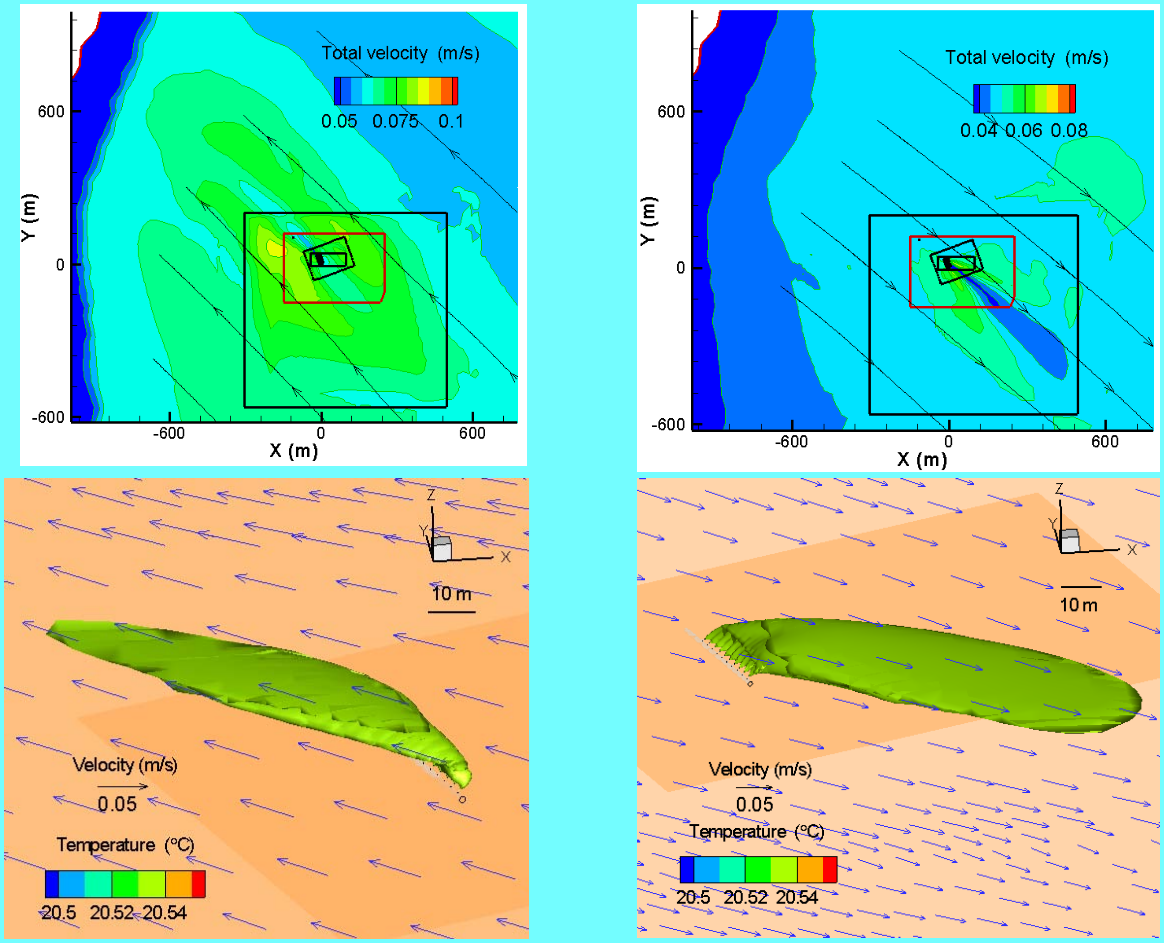

Solution for thermal discharge. Top – velocity field, bottom – 3D thermal plume and water surface vectors, left – flood tide, right – ebb tide.

Discharge into coastal flow --- solution movie

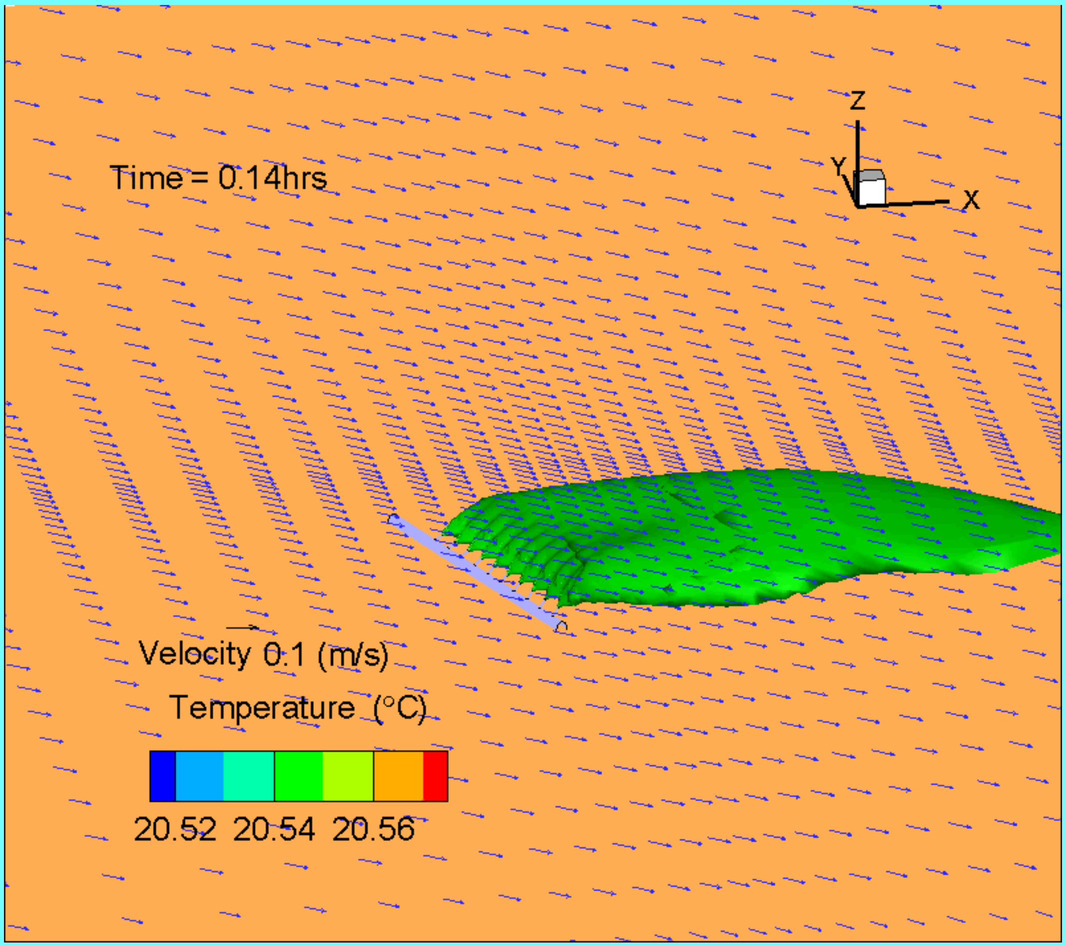

Animation of the temperature iso-surface under action of tides

Concluding remarks

Conclusion and Future work

1) Overset grid techniques are powerful in resolving multi-scale and multi-physics problems
2) A systematic investigation on accurate and stable model interface algorithms is necessary
3) Challenges: coupling between different sets of PDE and flow models

References

Wu and Tang, 9th Int. Conf. Hydro. Shanghai, China. Accepted. Oct. 11-15, 2010.
Tang, Paik, Sotiropoulos, and Khangaokar. J. Hydr. Eng, 2008.
Tang, Computers & Fluids., 2006.
Chen, Liu, and Beardsley, J. Atm. & Oceanic Tech., 2003.
Tang, Jones, and Sotiropoulos, J. Comput. Phys., 2003.
Tang and Zhou, SIAM J. Numer. Anal., 1999.

------------ Thanks ---------